

# Sensitivity analysis of input ground motion on surface motion parameters in high seismic regions: A case of Bhutan Himalaya

Karma Tempa<sup>1</sup>, Komal Raj Aryal<sup>2</sup>, Nimesh Chettri<sup>1</sup>, Giovanni Forte<sup>3</sup>, Dipendra Gautam<sup>4,5,6\*</sup>

<sup>1</sup>Civil Engineering Department, College of Science and Technology, Royal University of Bhutan, Phuentsholing, Bhutan

<sup>2</sup>Faculty of Resilience, Rabdan Academy, Abu Dhabi, United Arab Emirates

<sup>3</sup>Department of Civil, Environmental and Architectural Engineering (DICEA), University of Naples Federico II, Naples, Italy

<sup>4</sup>Department of Civil Engineering, Cosmos College of Management and technology, Lalitpur, Nepal

<sup>5</sup>Department of Civil Engineering, Institute of Engineering, Thapathali Campus, Kathmandu, Nepal

<sup>6</sup>Interdisciplinary Research Institute for Sustainability, Kathmandu, Nepal

\* *Correspondance*: Dipendra Gautam (dipendra01@tcioe.edu.np)

**Abstract.** Historical earthquakes demonstrate that strong motion characteristics and local soil condition, when coupled, significantly influence seismic site response. Interestingly, most of the Himalayan earthquakes depicted anomalous behavior per the site conditions historically. Being one of the most active seismic regions on earth, the eastern fringe of the Himalaya has observed many devastating earthquakes together with non-uniform damage scenarios. To quantify such anomalies, we evaluate surface motion parameters for a soft soil deposit located at Phuentsholing City in western Bhutan. Using one dimensional site response analysis, sensitivity of ground motion variation is estimated. This study accounts for the earthquakes of moment magnitudes 6.6 to 7.5 with a wide variation of peak ground acceleration (PGA). To dissect the characteristics of six inputted ground motions on eight local ground conditions, sensitivity analysis is performed statistically. The statistical correlation of the response data sets and the linear regression model of the bedrock outcrop and the surface motion spectral acceleration along the stratified depth are examined to quantify the variation in surface motion parameters. The results highlight that the strong motions with PGA greater than 0.34g demonstrate greater sensitivity, leading to some anomalies in response parameters, especially amplification. Similar results were obtained for the low PGA range ( $<0.1g$ ).

**Keywords:** seismic site effect, amplification factor, soil fundamental period, sensitivity analysis, Bhutan.

## 1. Introduction

Bhutan is located in the eastern fringe of Hindu-Kush-Himalaya. Historical earthquakes that occurred in the Hindu-Kush-Himalayan region have resulted in enormous losses and damages (Gautam et al., 2016). Akin to the historical earthquakes, the impending earthquakes are certain to strike the region and result in detrimental consequences. The eastern fringe of Himalaya, i.e., Bhutan, and neighboring areas were strongly shaken by significant earthquakes in the past; however, most of the earthquakes that occurred until the 18<sup>th</sup> century are not well documented. The most recent events such as the April 05, 2021 ( $M_w$  5.0) in Samtse (South Bhutan) and the

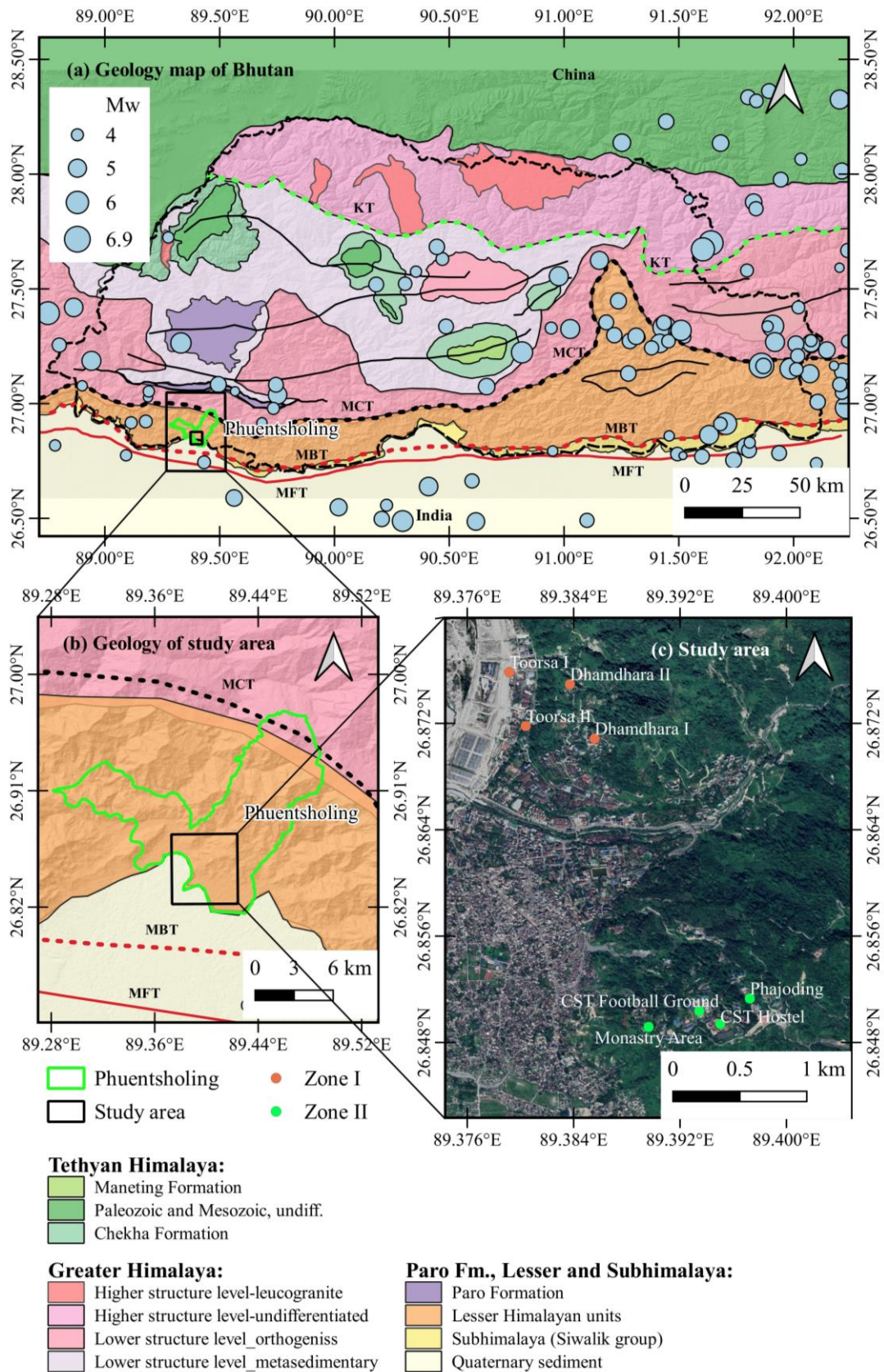
36 September 2009 Mongar earthquake ( $M_w$  6.7) in eastern Bhutan manifested widespread damage to Bhutan and  
37 neighboring regions. These earthquakes caused major damages in the eastern parts of Bhutan and considerably  
38 affected the other parts of the country (Chettri et al., 2021a, b). All the past earthquakes highlighted anomalous  
39 damage pattern to structures and infrastructures in various parts of the country, especially in the plain areas. This  
40 evidence indicates the likely local site effect in Bhutan. So far, few studies on local seismic response are in  
41 Bhutan, using a single strong motion record, but the reported studies mainly focus on the role of bedrock depth  
42 in ground response parameters (Tempa et al., 2020; Tempa et al., 2021). The ground motion response analysis  
43 may not adequately address the accuracy in predicting the response when the information is limited regarding  
44 site characteristics and their variations within the same soil column (Stevens et al., 2020). In the case of data  
45 scarce regions such as Bhutan, the variation in terms of material characteristics can be possibly accounted for  
46 using sensitivity analysis. For this reason, this study quantifies the characteristics and effects of several strong  
47 ground motions. Seismic ground response analysis fall in the Grade III approach of microzonation studies (e.g.  
48 ISSMGE 1999; Licata et al., 2018). It is widely used method by researchers for various applications in order to  
49 capture local ground effects or site conditions that can affect the estimate of ground motion characteristics  
50 (Chavez-Garcia et al., 1990; Lopez-Caballero et al., 2012; Gautam & Chamlagain, 2016; Sil & Haloi, 2018).  
51 The outcomes of such studies aim to provide local seismic hazard parameters, which can be adopted for design  
52 of structures and infrastructures (Douglas, 2006). Ground response parameters typically characterize the  
53 complex nature of strong motion accelerograms using a simple expansion of predictive relationships. Two  
54 prominent approaches, deterministic and probabilistic, are widely used for seismic hazard studies. Tempa et al.  
55 (2021) recommended the use of the deterministic approach that can estimate the parameters under various  
56 earthquake occurrence scenarios. Notably, selecting a single ground motion considering amplitude for seismic  
57 site response analysis may not be a reliable approach to estimate site amplification. Selection of a wide  
58 amplitude range and the assessment of likely fluctuation scenario for Bhutan is not done yet. Hence, ground  
59 motion parameters that are related to the amplitude are investigated to examine and predict the variability, often  
60 regarded as sensitivity, concerning mean values and associated scatter.

61 In this paper, sensitivity analysis of site response for specific soil conditions in Phuentsholing, Bhutan is  
62 explored by a statistical correlation function of the ground motion parameters for different earthquake shaking  
63 intensities. The study area is one of the major urban and commercial hubs in Bhutan Himalaya and seismic site  
64 effects on existing structures may have detrimental consequences due to inherent vulnerabilities of structures  
65 and infrastructures as well as due to the likely phenomenon such as amplification in loose soil deposits. To  
66 quantify the seismic site effects in terms of amplification of amplitude parameters, a range of time histories is  
67 selected, and site response parameters are estimated.

## 68 **2. Seismicity and geology of the study area**

69 Himalaya is one of the most seismically active regions on earth, which observes both large and  
70 moderate-sized events frequently (Drukpa et al., 2006). Bhutan is located in the eastern Himalayas formed due  
71 to the subduction of the Indian Plate beneath the Eurasian Plate and spans from the low-lying Brahmaputra Plain  
72 to the high Tibetan Plateau. Most of the land area of Bhutan is underlain by the Main Himalayan Thrust (MHT),  
73 which runs along the entire length of the Himalayan arc. Historical earthquake catalog (see Fig. 1a) indicates  
74 that Bhutan has experienced several earthquakes of moment magnitude greater than 5 since early 1900, among  
75 them, the 1915 Trashigang ( $M_w$  6.6), 1954 Trashiyangtse ( $M_w$  6.4), and the 2009 Mongar ( $M_w$  6.1) earthquakes

76 are the most notable ones. The 2011 Sikkim-Nepal earthquake ( $M_w$  6.9) also caused noticeable damage to  
77 building stocks in Bhutan (Chettri et al., 2021a). The earthquakes in the vicinity of the study area  
78 (Phuentsholing) include the 1981 Dagana ( $M_w$  5.1) earthquake and the 2003 Haa earthquake ( $M_w$  5.5). The most  
79 recent event occurred in Samtse in 2021 ( $M_w$  5.1) affected Phuentsholing and the neighboring areas with an  
80 intensity level of IV in Modified Mercalli Intensity (MMI) scale (Gautam et al., 2022). Continuity of seismic  
81 activities in Bhutan is attributed to the presence of major shear zones such as the Main Himalaya Thrust (MHT),  
82 Main Boundary Thrust (MBT), Main Central Thrust (MCT), and the South Tibetan Detachment System (STDS)  
83 (Long & McQuarrie, 2010) as shown in Fig. 1a. The study area is within the Phuentsholing Formation of Buxa  
84 group of the Lesser Himalaya, mainly characterized by highly weathered dark grey to black slate and phyllite,  
85 thin interbedding of limestone with substantial amount of cream-colored dolomite and fine-medium quartzite,  
86 additionally consisting fine to medium grained conglomeratic quartzite interbedded with phyllite and dolomite  
87 towards the Rinchending area of Zone II. Hence, the lithological characteristic of the area indicates weak and  
88 highly unstable geology in the region. The presence of thrust faults in the proximity of the study area along the  
89 entire belt of the Lesser Himalayan units and the quaternary sediments in the south depict the area to be  
90 seismically active with the majority of the historical earthquake events concentrated within these geological  
91 units. In particular, this study focuses on Phuentsholing city of Chhukha district in Bhutan (Fig. 1c). The city is  
92 one of the major commercial hubs for trade with India. The study area is observing rapid infrastructure  
93 development activities and urban expansion for residential, commercial, and industrial purposes. Phuentsholing  
94 city covers an area of 15.6 km<sup>2</sup> and is located at 26.86°E and 89.39°N. The city has the population of 27,658,  
95 mostly distributed towards the peripheral international border area with a total of 2,263 residential and  
96 commercial buildings per the 2020 statistics (<http://www.pcc.bt/index.php/>). The seismic site characterization  
97 includes eight locations in the regions of Dhamdhara, Toorsa, and Rinchending in Phuentsholing, Bhutan. In  
98 this study, the sites are grouped into two main zones based on the geographical location and immediate  
99 availability of survey locations. These two zones also refer to the Local Area Plan (LAP) of Phuentsholing. The  
100 zones are Zone I: Dhamdhara I, Dhamdhara II, Toorsa I, and Toorsa II, and Zone II: College of Science and  
101 Technology (CST) Football Ground, CST Hostel, Phajoding, and the Monastery area. Among the 8 LAPs,  
102 Dhamdhara and Toorsa (Zone I) are in the same region in the western part of the city and Rinchending (Zone II)  
103 is in the east.



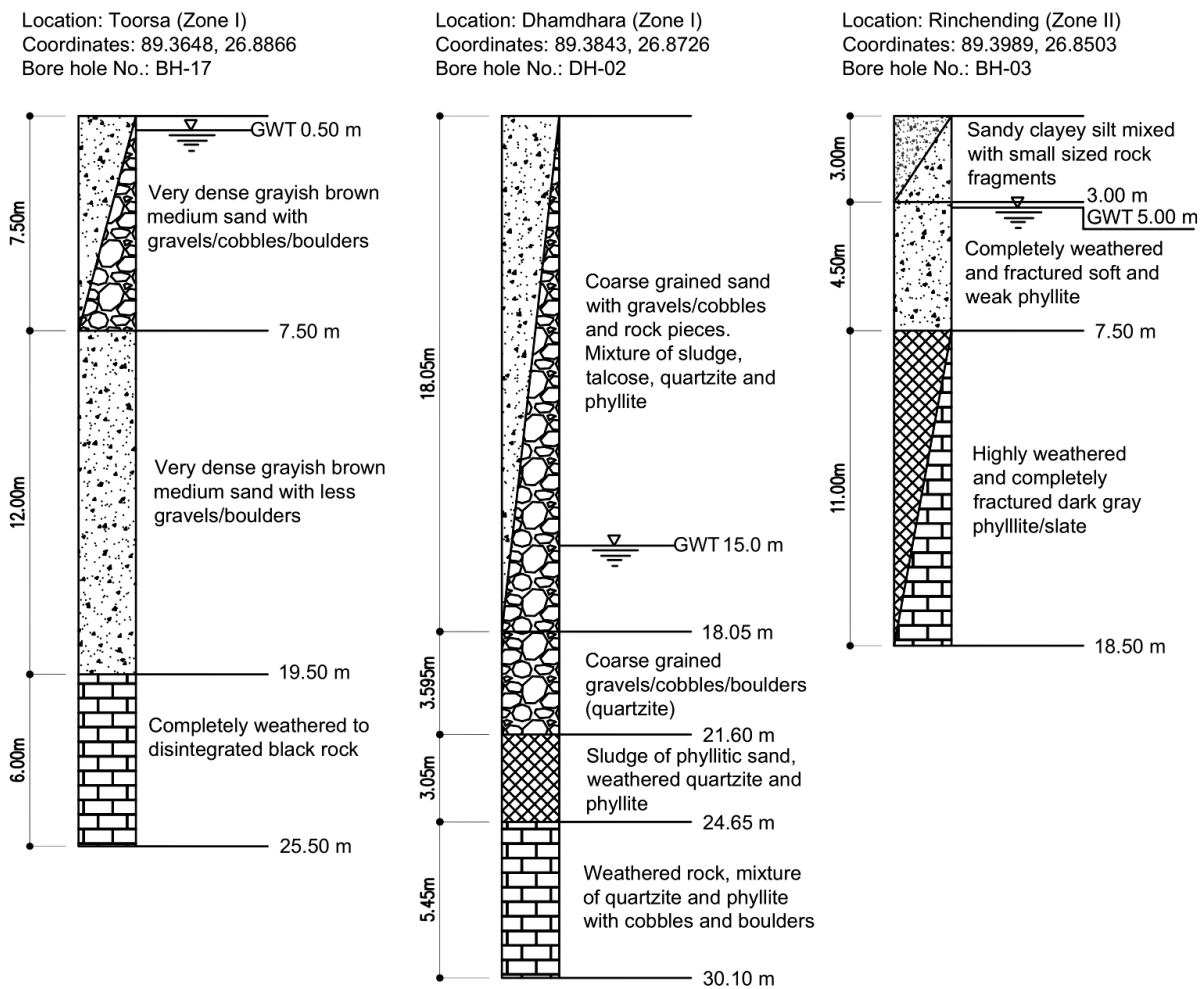
104

105 **Figure 1:** Geology and seismicity and the study area: (a) Geological map of Bhutan reproduced from McQuarrie  
 106 et al. (2013) and seismicity, (b) Location of Phuentsholing and geology of the area, (c) Study area showing  
 107 surveyed site using MASW (modified from Google Earth Pro 2021).

108 **3. Materials and method**

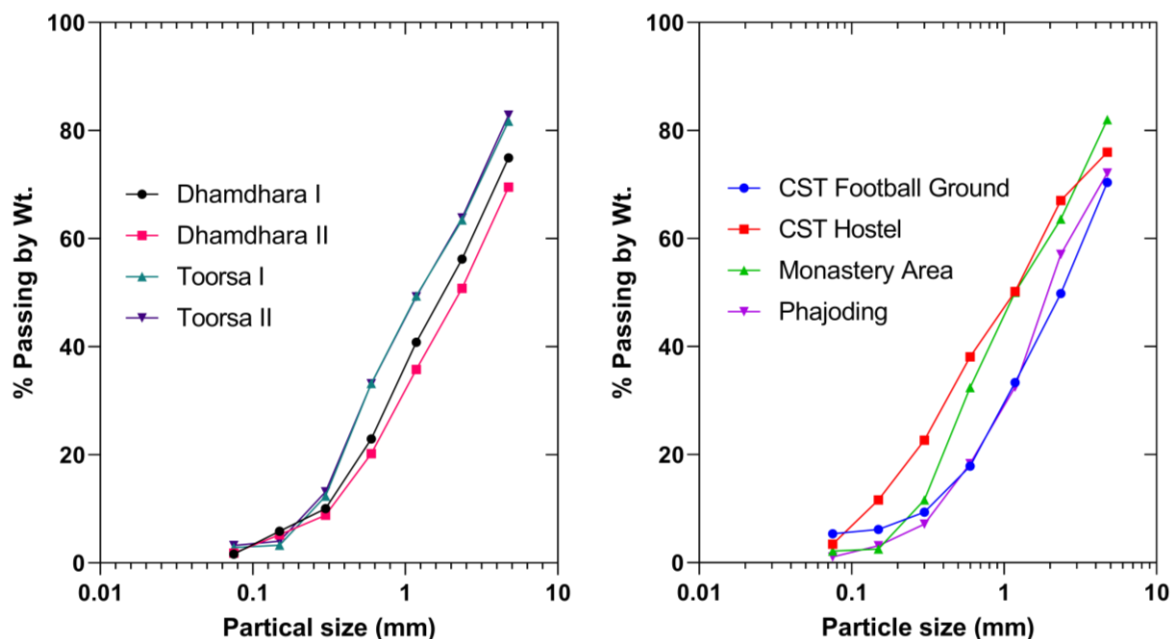
109 **3.1 Geotechnical site characterization**

110 The geotechnical reports collected by Phuentsholing municipality have 29 stratigraphic logs. From  
 111 these records, the depth of the water table (GWT) was demarcated first. Drilling log data showed the highest  
 112 depth of the water table in the Dhamdhara area at 12.5 m to 16 m, whereas groundwater table in Rinchening  
 113 area is at 5 m, followed by the Toorsa area at 0.5 m and 3 m, which is located near the riverbed. The depth of the  
 114 water table is one of the essential input parameters used for 1D ground response analysis. Three drill holes are  
 115 presented to illustrate the typical underground stratigraphy (Fig. 2). Table 1 presents a summary of soil  
 116 properties from laboratory testing of in-situ samples collected from the drill holes. The number of samples in  
 117 each zone represents the total number of samples collected from all drill logs at various stratigraphic depths. All  
 118 laboratory tests have been verified according to the Indian Standard Codes. Testing included physical  
 119 identification, Atterberg limits, grain size distribution and direct shear testing. Field tests such as standard  
 120 penetration resistance (SPT) and core cutter test were performed to determine resistance to penetration (SPT-N)  
 121 and field density, respectively



122  
 123 **Figure 2:** Typical borehole stratigraphy in Toorsa and Dhamdhara (Zone I) and Rincheningding (Zone II).

124 As shown in the stratigraphic logs, the upper stratum comprises predominantly mixed coarse-grained  
 125 soils characterized by considerable fraction of sand. The soil classification of the Phuentsholing area carried out  
 126 by sieve analysis highlighted that most soils consist of 22.74% gravel, 74.89% sand, and 2.37% of the silt and  
 127 clay. The sieve analysis results for the respective zones are shown in Fig. 3. The soils in Toorsa are non-plastic,  
 128 as coarse-grained soils dominate the particle distribution, while the soils in Rinchending and Dhamdhara have  
 129 low plasticity with a plasticity index (PI) of 6.5 and 10, respectively. The bulk density is 1.8 g/cm<sup>3</sup> in Toorsa,  
 130 1.64 g/cm<sup>3</sup> in Dhamdhara, and 1.33 g/cm<sup>3</sup> in Rinchending. The shear strength parameter, cohesion (c), ranges  
 131 between 0-0.18 kg/cm<sup>2</sup>, while the angle of internal friction ( $\phi$ ) in the study area is up to 35°.



132  
 133 **Figure 3:** Representative grain size distribution curve for the study area.

134 **Table 1.** Average soil parameters in the study area.

Location	Testing methods	Soil parameters	No. of samples	Reference
Toorsa (Zone I)	Atterberg's limit	Non-plastic	86	IS: 2720 (Part 5)-1995
	Core cutter	Bulk density, $\gamma_t = 1.8$ g/cc Dry density, $\gamma_d = 1.64$ g/cc		IS:2720 (Part 29)-1975
	Direct shear	$c = 0$ $\phi = 35^\circ$		IS: 2720 (Part 13)-1997
	SPT	$N$ -value = 25 to 50		IS: 2131-1981
Dhamdhara (Zone I)	Atterberg's limit	Low plasticity (PI = 6.5)	28	IS: 2720 (Part 5)-1995
	Core cutter	Bulk density, $\gamma_t = 1.64$ g/cc Dry density, $\gamma_d = 1.51$ g/cc		IS:2720 (Part 29)-1975
	Direct shear	$c = 0.073$ kg/cm <sup>2</sup>		IS: 2720 (Part 13)-1997

		$\phi = 31.44^\circ$		
	SPT	$N$ -value = 19 to 37		IS: 2131–1981
Rinchending (Zone II)	Atterberg's limit	Low plasticity (PI = 10)	26	IS: 2720 (Part 5)-1995
	Core cutter	Bulk density, $\gamma_s = 1.83$ g/cc Dry density, $\gamma_d = 1.70$ g/cc		IS:2720 (Part 29)-1975
	Direct shear	$c = 0.18$ kg/cm <sup>2</sup> $\phi = 20$ -30°		IS: 2720 (Part 13)-1997
	SPT	$N$ -value = 21 to <100		IS: 2131–1981

135

136

137

138

139

140

141

142

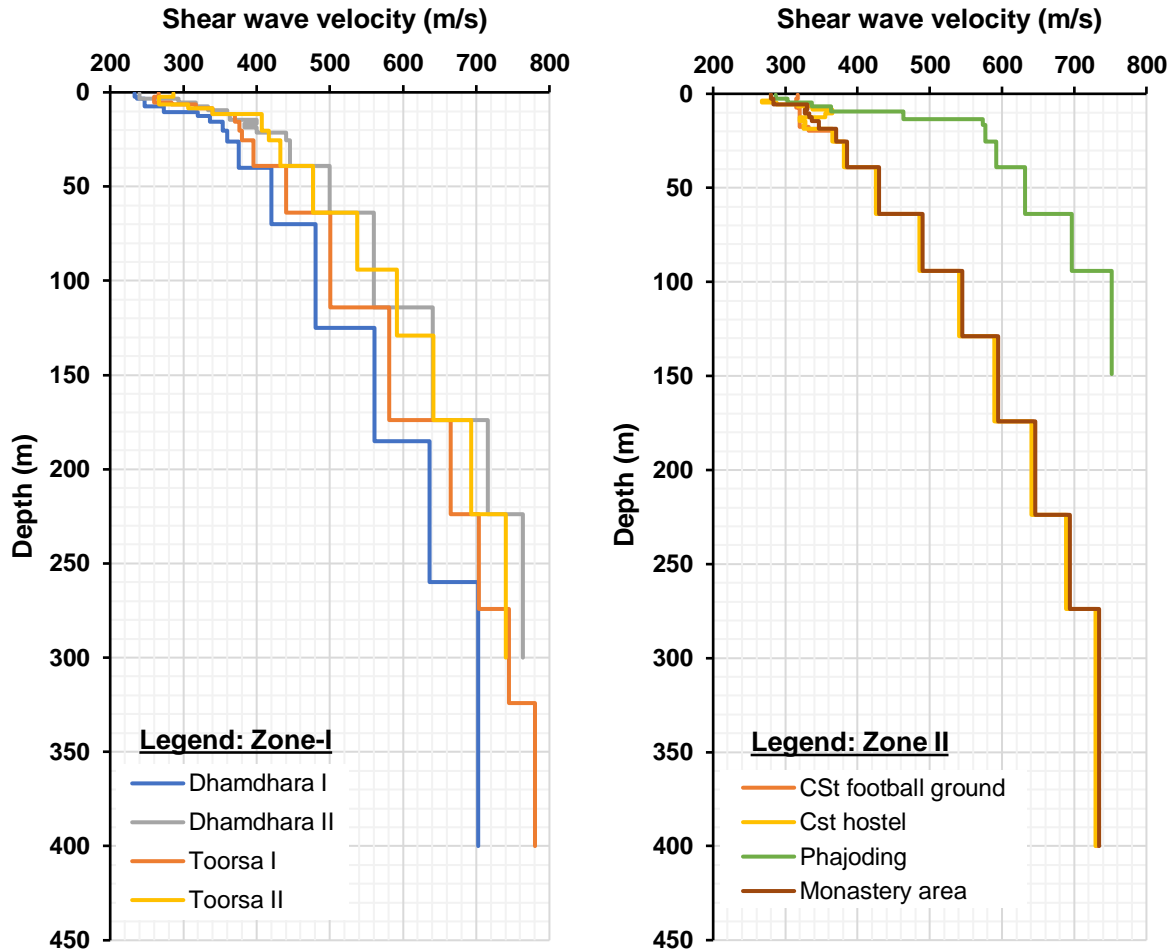
143

Shear wave velocity profiles from eight locations in the study area based on the multispectral surface wave analysis (MASW) and empirical correlation developed by (Tempa et al., 2021) are used for input parameters. According to the shear wave velocity profile, engineered bedrock ( $V_s > 800$  m/s) lies at a depth of 150 m to 400 m as shown in Fig. 4. According to the parametric analysis carried out by Tempa et al. (2020), the site condition in the study area is classified as ground type B per the Euro Code EC-08 and National Earthquake Hazards Reduction Program (NEHRP) with the majority of shear velocity ( $V_{s,30}$ ) values falling between 380–470 m/s, except for Phajoding, which has shear wave velocity of 584.76 m/s (Table 2).

**Table 2.** Site classification as per Euro Code EC-08

Zones	Sites	$V_{s,30}$ (m/s)	Ground Type
I	Dhamdhara I	386.43	B
	Dhamdhara II	435.92	B
	Toorsa I	439.54	B
	Toorsa II	464.30	B
	CST football ground	426.76	B
II	CST hostel	426.61	B
	Monastery area	446.20	B
	Phajoding	584.76	B
All	Bedrock	>800	A



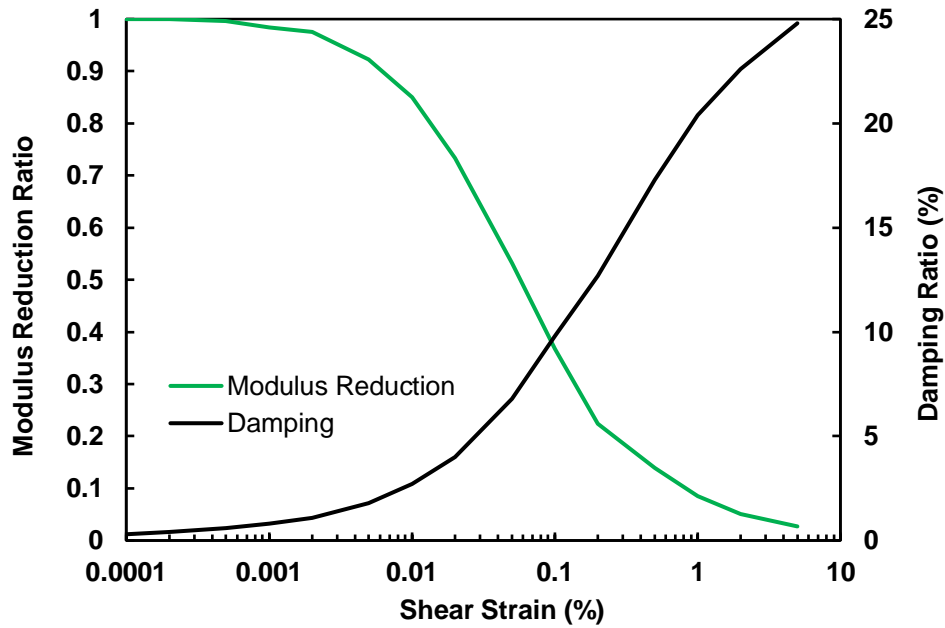


144

145 **Figure 4:** Shear wave velocity profile of study locations in Phuentsholing, Bhutan.

146 Dynamic properties of soils are influenced by shear modulus and damping and are defined by the  
 147 respective degradation models, regarded as the backbone curves. Fig. 5 represents the dynamic soil model for  
 148 sand used in this study. Degradation models are well established by many investigators for different types of  
 149 soils (see e.g., Seed & Idriss, 1970; Vucetic & Dobry, 1991; Darendeli, 2001; Dobry & Vucetic, 1982; Seed et  
 150 al., 1986). A damped linear elastic model of the soil system is used for the analysis. Due to soil nonlinearity for  
 151 which the shear modulus is strain dependent, ProShake performs an iterative process on the linear model until  
 152 both the moduli and damping ratios are compatible with the average strains and convergence is achieved at the  
 153 last iteration (Shafiee et al., 2011; Puri et al., 2018). The nonlinear and hysteretic stress-strain behavior of soils  
 154 under cyclic loading is approximated as a function of  $G_{sec}$  and  $G_{max}$ . The predetermined estimation of  $G_{sec}$  or  $G$   
 155 and  $G_{max}$  is attributed to unit weight or bulk density,  $\rho$ , and shear wave velocity,  $V_s$  ( $G_{max} = \rho V_s^2$ ). Similarly,  
 156 damping ratios are predicted as a function of  $G_{sec}$  or  $G$  values. This estimation is achieved using an iterative  
 157 procedure in the Proshake 2.0 program (EduPro Civil Systems Inc., 2017).





158

159 **Figure 5:** Average modulus reduction ratio and damping ratio adopted for sand (Seed & Idriss, 1970).

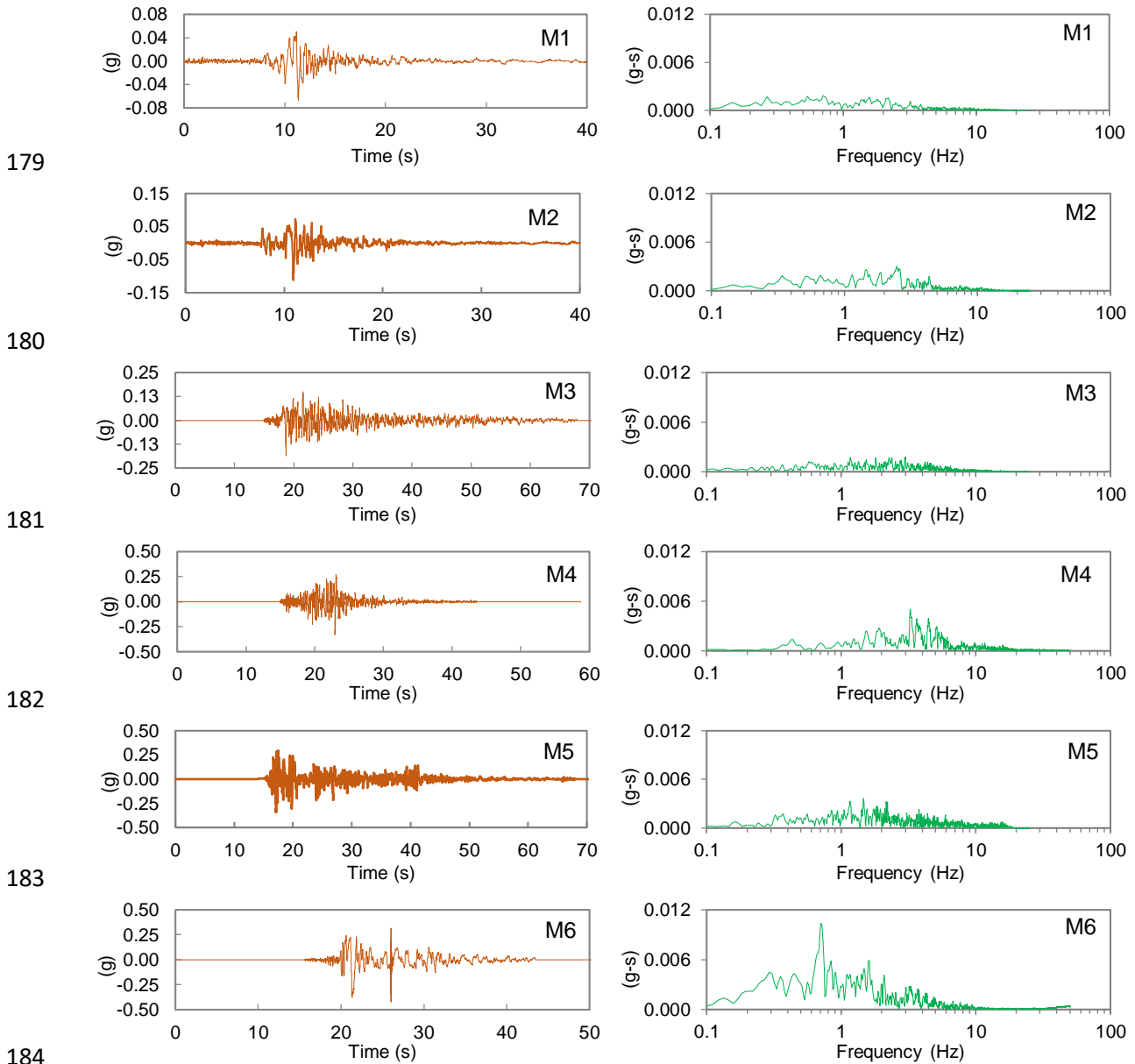
160 **3.2 Selection of input motion**

161 Definition of the input motion that is considered for site response analysis of an area requires both subsurface  
 162 characterization and careful selection of acceleration time histories. In Bhutan, records of acceleration time  
 163 histories are very rare, if not absent. In the absence of a national seismic code, Bhutan is assumed to fall under  
 164 Indian seismic zone IV and V, with an expected maximum PGA of 0.24 g and 0.36 g for design purposes. For  
 165 these two zones, the PGA for earthquakes with a return period of 475 years is expected to be half of the  
 166 maximum considered earthquake (MCE), i.e., 0.12 g and 0.18 g. Notably, the GSHAP depicts the PGA range  
 167 between 0.2-0.28g with an increasing trend towards the east of the country. Considering the variations in  
 168 expected PGA, we selected six acceleration time histories as input motions with PGA ranging from 0.067 g to  
 169 0.422 g, considering the lowest and the highest range of possible earthquake scenarios (Table 3). The  
 170 acceleration time histories used for the 1D ground response analysis are shown in Fig. 6 in ascending PGA order  
 171 using the ProShake 2.0 computer program. In the ProShake 2.0 program, input motion and soil profile are  
 172 denoted as “M” and “P”, respectively, and are annotated in the subsequent sections (Table 3). The amplitude  
 173 and frequency content of the bedrock level motion are particularly the most important parameters (Kirtas et al.,  
 174 2015; Kramer, 1996). To understand the strong ground motion characteristics, we plotted the Fourier amplitude  
 175 versus period in the frequency domain, representing the Fourier amplitude spectra of the input motions, as  
 176 shown in Fig. 6. The effect of local soils is indicative at a much higher frequency range in all the investigated  
 177 sites.

178 **Table 3.** Selected strong motion records for ground response analysis.

Event	Station	Year	$M_w$	PGA (g)	Notation
Loma Prieta/Santa Cruz Mountains	Yerba Buena Island, CA – US	1989	6.9	0.067	M1
Loma Prieta	Diamond Heights	1989	6.9	0.113	M2

Taft Kern County	Taft	1952	7.5	0.185	M3
Northridge	Topanga Fire Station	1994	6.7	0.329	M4
El Centro	Imperial Valley Irrigation District	1940	6.9	0.344	M5
Petrolia	Cape Mendocino	1992	6.6	0.422	M6



185 **Figure 6:** Strong motions and corresponding Fourier amplitude plots of the input ground motions.

### 186 3.3 1D ground response analysis

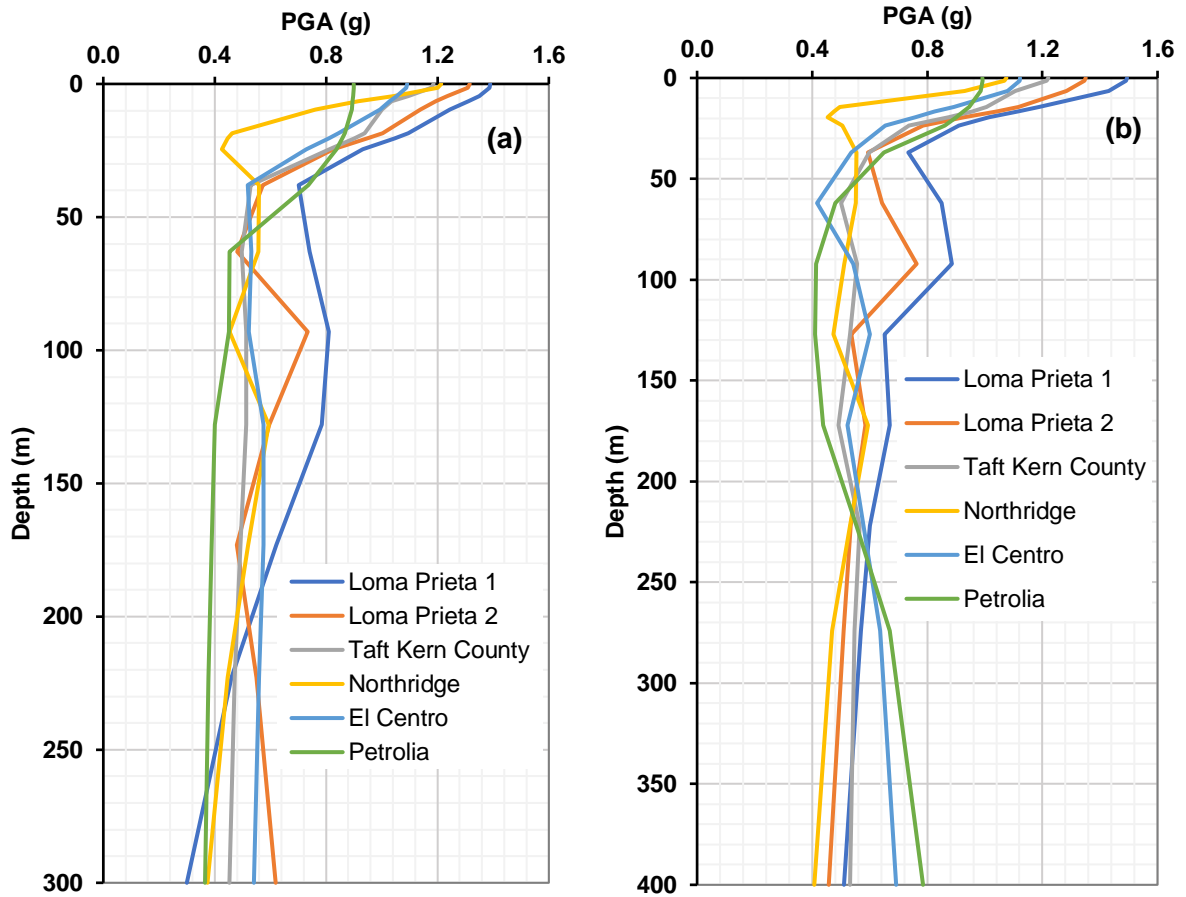
187 One dimensional equivalent linear analysis is performed at eight sites in Phuentsholing, Bhutan to estimate local  
188 site effects using the ProShake 2.0 program. In this study, six strong motion records are used to represent low,  
189 medium, and high acceleration categories. The ProShake 2.0 program provides the flexibility to input ground  
190 motions and soil profiles and is useful for estimating the outcrop responses to input ground shaking. The  
191 improved shear wave velocity profiles down to the engineered bedrock depth (150 m and 400 m) from eight

192 sites are used. The deep shear wave profiles used in this study incorporate the effects of depth and soil type of  
193 visco-elastic soil layers above the predicted engineering bedrock. The 1D ground response analysis accounts for  
194 wave propagation from the bedrock outcrop through the visco-elastically stratified soil deposit and provides an  
195 estimate of the surface motion parameters. The complex response method is solved by the equation of motion in  
196 the frequency domain. Nonlinear soil response is estimated by an iterative quasi-linear procedure in which  
197 successive linear analyses are performed while updating the shear modulus and damping ratio based on the  
198 shear strain level obtained from the preceding iteration. Iterations continue until the strain-compatible modulus  
199 and damping converge.

## 200 **4. Results and discussion**

### 201 **4.1 Seismic site effects**

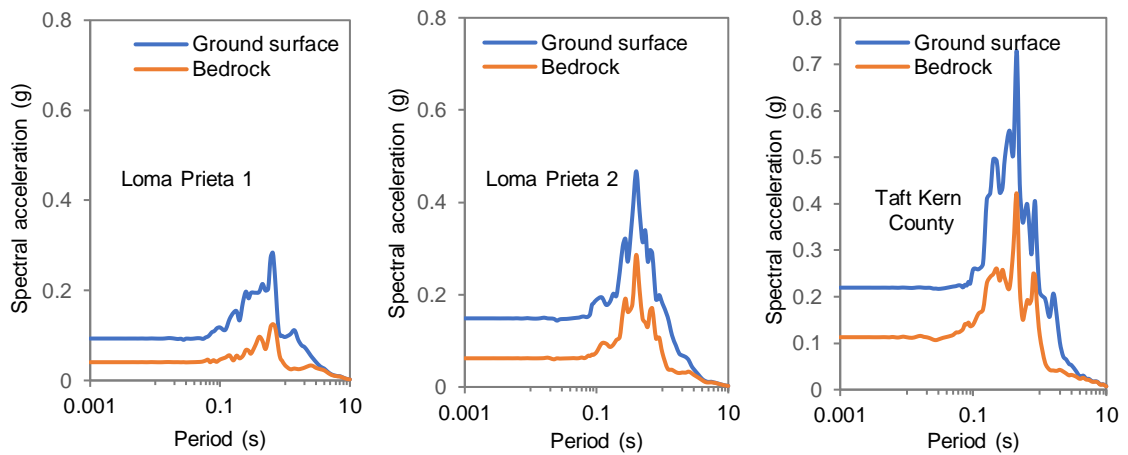
202 Fig. 7 shows normalized PGAs on surface at two typical locations of the investigated zones. The chart shows  
203 PGA of 1.2 g to 1.5 g for low PGA earthquakes and 0.7 g to ~1.1 g for medium and high PGA earthquakes.  
204 Response parameters can be defined and characterized based on the amplitude parameters of the ground motion  
205 and the severity of the ground motion excitation in nearby structures. This, in turn, is a function of the  
206 amplitude or intensity, the frequency content, and the duration of the ground motion (Bradley, 2011). Natural  
207 periods or frequency domain parameters are related to the seismic behavior of structures and indirectly reflect  
208 the ground motion characteristics (Zafarani et al., 2020). Hence, to commensurate this relationship, the response  
209 spectra of bedrock and surface motion are presented in Figs. 8 and 9, respectively. The results of various input  
210 ground motions indicate the higher spectral acceleration of the soil profile in the period range between 0.3 s to  
211 3.0 s, with the peak spectral acceleration range of 0.14 g to 1.62 g. Thus, the structures with similar fundamental  
212 vibration periods are likely to be exposed to greater peak spectral acceleration.



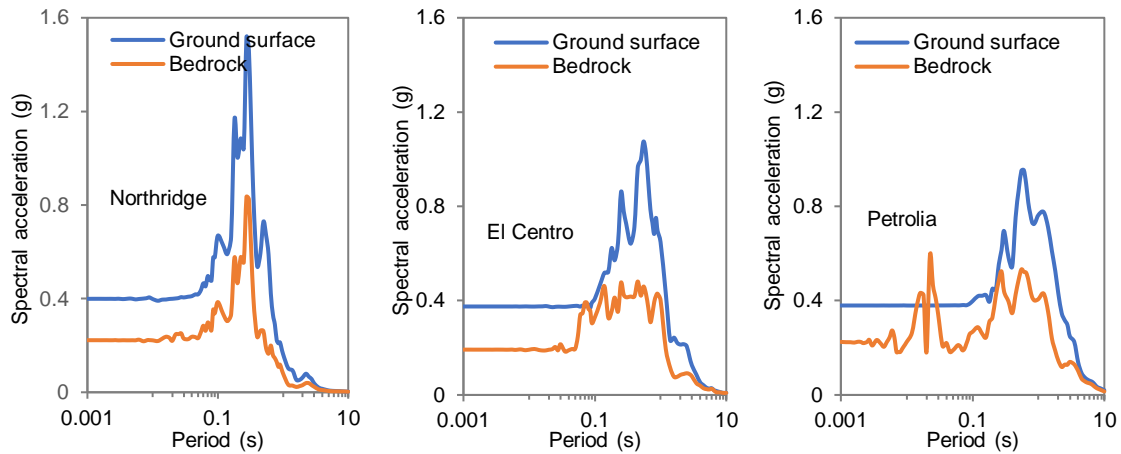
213

214 **Figure 7:** The typical profiles of normalized peak ground acceleration (PGA), (a) Toorsa II in Zone I, and (b)

215 CST Football Ground in Zone II.

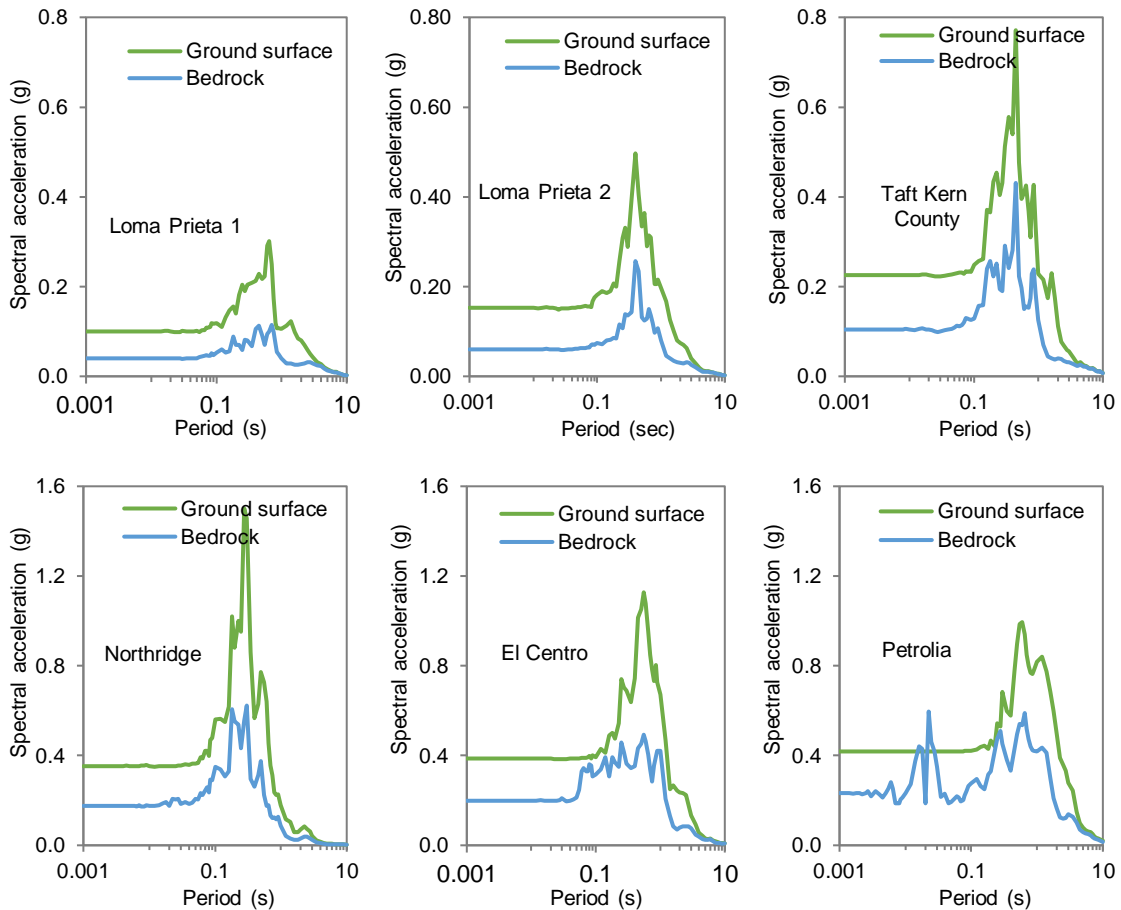


216



217

218 **Figure 8:** Typical spectral acceleration of bedrock and ground surface motion at Toorsa II in Zone I  
 219 corresponding to the respective input motions.

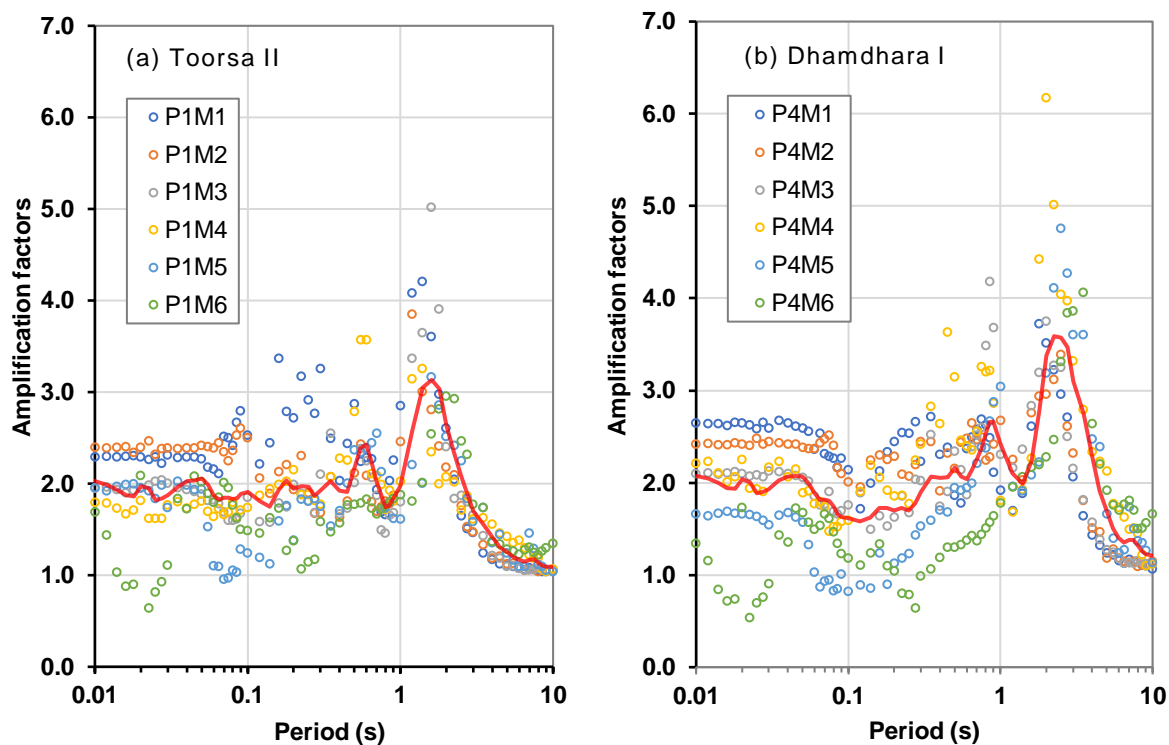


220

221  
 222 **Figure 9:** Typical spectral acceleration of bedrock and ground surface motion at CST Football Ground in Zone  
 223 II corresponding to the respective input motions.

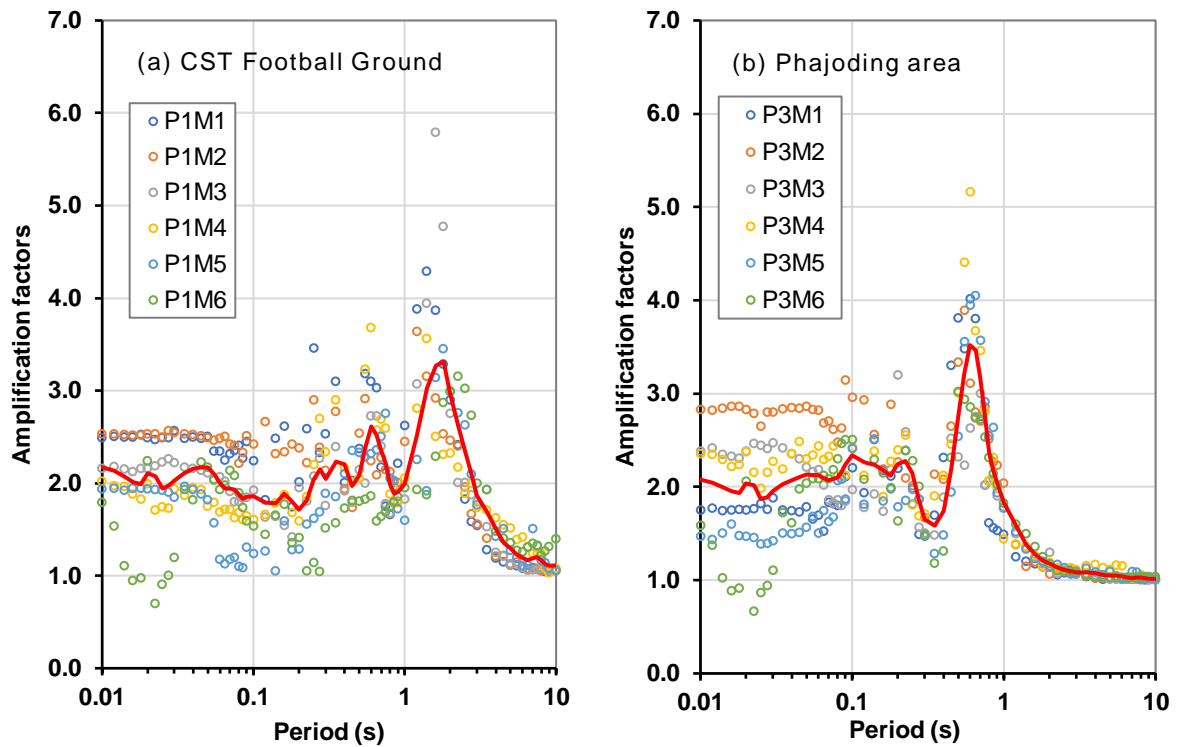
224 Figs. 10 and 11 show the results of typical amplification factors at two locations in the study area. The  
 225 amplification factors range from 0.7 to 2.7, 0.6 to 2.6, 0.75 to 2.5, and 0.7 to 3.2 for Toorsa II, Dhamdhara I,  
 226 CST football ground, and Phajoding, respectively for 0.01 s to 0.1 s natural period. In the period range from 0.1

227 to 1.0 s, the amplification factors are in the range from 1.1 to 3.6, 0.7 to 4.2, 1.0 to 3.7, and 1.2 to 5.2 for Toorsa  
 228 II, Dhamdhara I, CST football ground, and Phajoding, respectively. In the natural period range, the  
 229 amplification factors are 5.0, 6.2, and 5.8 for Toorsa II, Dhamdhara I, and CST football ground, respectively.  
 230 However, in the Phajoding the amplification factor is ~ 1.7 due to a much stiffer soil deposit ( $V_{s,30} = 584.76$  m/s)  
 231 and shallow engineering bedrock at 150 m.



232

233 **Figure 10:** Examples of amplification factors for various earthquakes at (a) Soil profile P1 at Toorsa II in Zone  
 234 I, (b) Soil profile P4 at Dhamdhara I in Zone I.



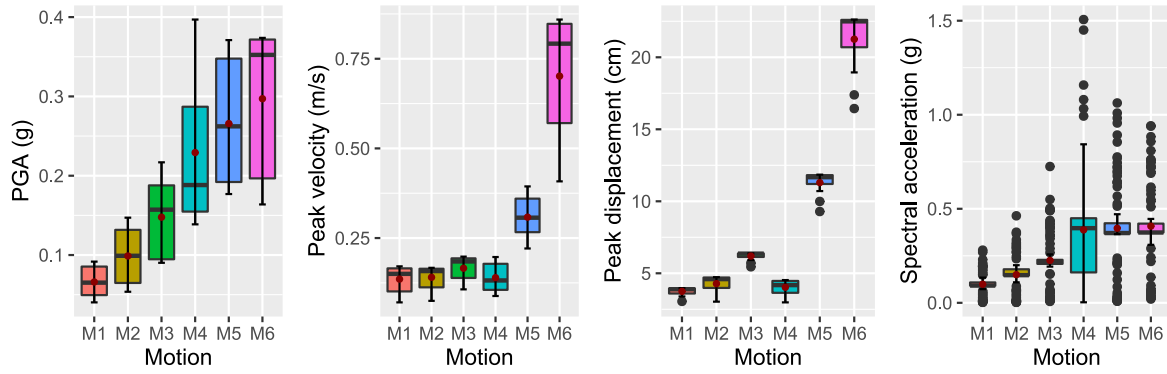
235

236 **Figure 11:** Examples of amplification factors for various earthquakes at (a) Soil profile P1 at CST Football  
 237 Ground in Zone II, (b) Soil profile P3 at Phajoding in Zone II.

238 **4.2 Correlation analysis**

239 The main objective of this study is to demonstrate the sensitivity of input motion amplitudes to predict the  
 240 variability of seismic site effects due to local ground conditions. We examined the potential trends, patterns, and  
 241 relationships between data sets for the numerical results. Using statistical analysis, variation of amplitude  
 242 parameters is projected by box plots (Figs. 12 and 13). Statistical correlations are fitted between peak ground  
 243 acceleration (PGA), peak ground velocity (PGV), peak ground displacement (PGD), and spectral acceleration  
 244 ( $S_a$ ) to determine the correlation between the effects of strong ground motion and the local soil conditions. As  
 245 anticipated, the 1992 Petrolia earthquake with 0.422 g PGA ( $M_w = 6.6$ ) led to the greatest response. However,  
 246 the 1994 Northridge earthquake with a PGA of 0.329 g ( $M_w = 6.7$ ) shows greater variability in spectral  
 247 acceleration compared to other earthquakes. This is because the spectral acceleration corresponds the interaction  
 248 between the ground and the shaking intensity of an earthquake. Therefore, from the perspectives of seismic site  
 249 effects the box plot of the spectral acceleration (period or frequency domain) is highly scattered with the  
 250 outliers, confirming uncertainty in the ground response characteristics in both regions. The El Centro and  
 251 Petrolia earthquakes, with the highest PGAs, also appear to be closely associated with spectral acceleration.

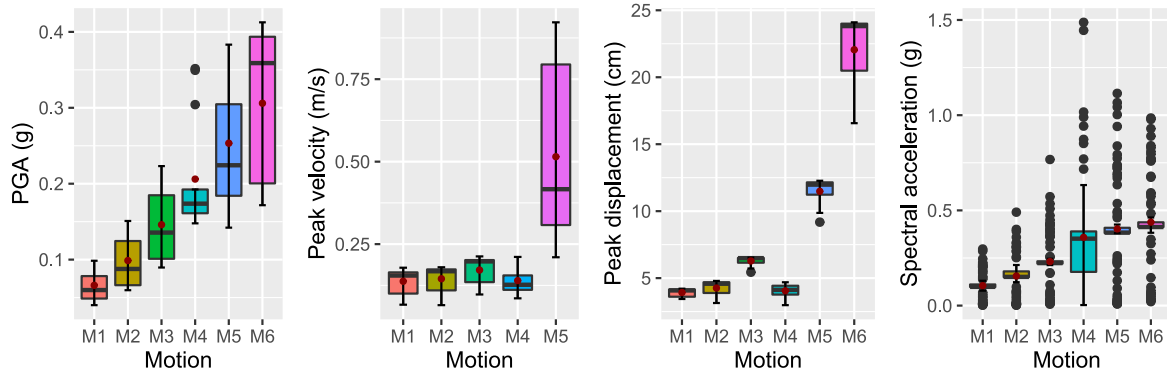




252

253

**Figure 12:** Box and whisker plot for ground motion parameters of soil profile at P1 Toorsa II in Zone I.



254

255

256

**Figure 13:** Box and whisker plot for ground motion parameters of the soil profile at P1 CST Football Ground in Zone II.

257

258

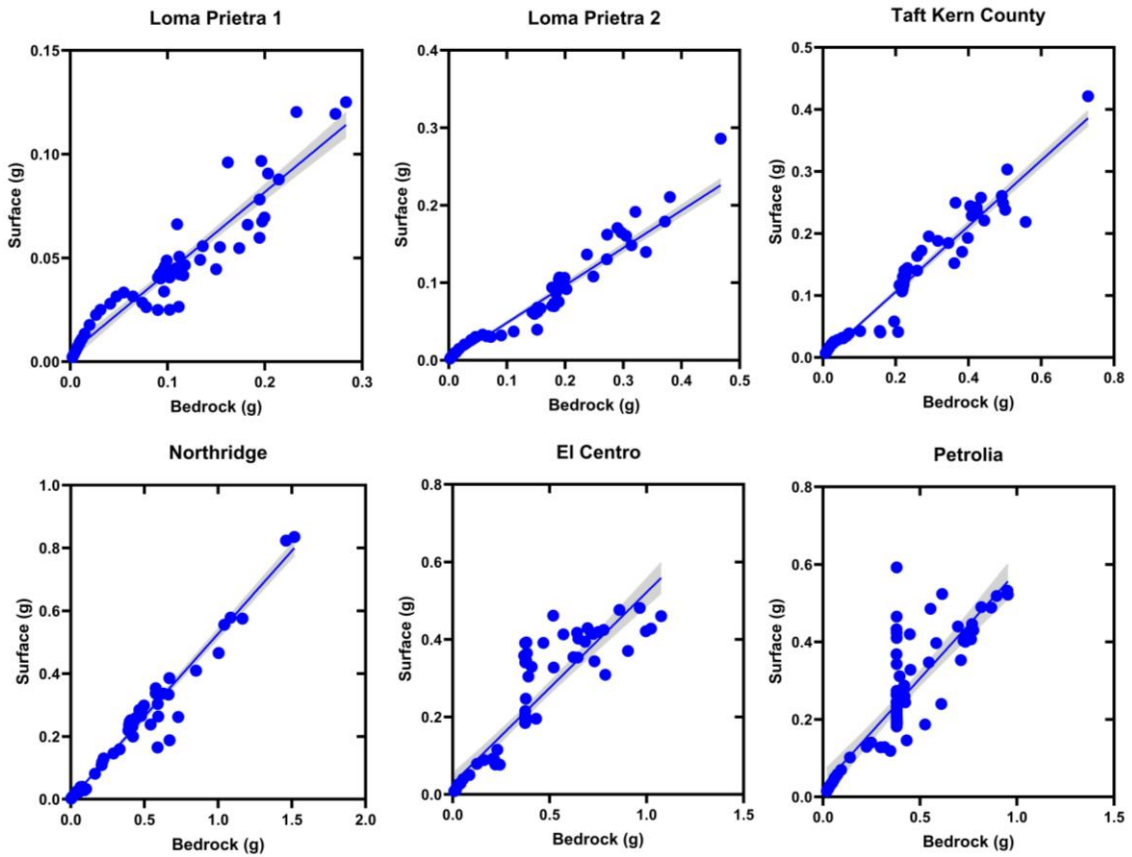
259

260

261

262

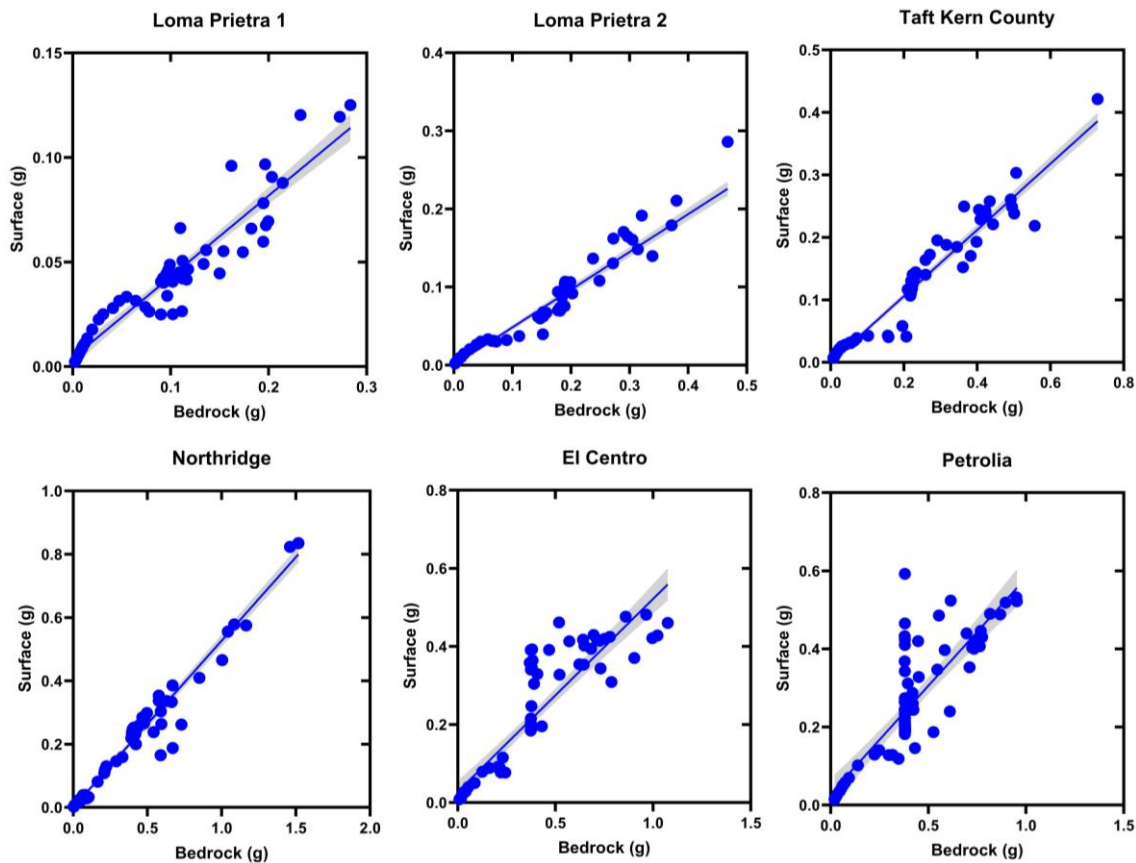
Primarily, propagating energy waves (outcrop motion) act on each stratified soil layers that amplifies or de-amplifies the ground motion response parameters at each layer. The sensitivity of the input motion parameters is critically monitored, and enhanced correlations are developed. To outline this, a linear regression model for bedrock outcrop motion and the predicted motion parameters as a function of bedding depth is developed. Regression analysis is performed for one particular soil profile from two zones (Toorsa II and CST Hostel) to substantiate sensitivity analysis (Figs. 14 and 15).



263

264 **Figure 14:** Linear regression model for bedrock and surface spectral accelerations for Toorsa II (Zone I).

265 The 95% confidence interval (CI) shows a linear relationship for the Loma Prieta 2, Taft Kern County, and  
 266 Northridge earthquakes indicate a closer impact on surface motion that corresponds the outcrop motion. In this  
 267 case, the predominant frequency content of the input motion is between 1 and 10 Hz. In contrast, the Loma  
 268 Prieta 1, El Centro, and Petrolia earthquakes, with a predominant frequency between 0.3 and 1.2 Hz, exhibit  
 269 typical nonlinearity throughout the spectral range, indicating possible damping of the spectral responses of the  
 270 soil deposits.



271

272 **Figure 15:** Linear regression model for bedrock and surface spectral accelerations for CST Hostel (Zone II)  
 273 Sensitivity of input motion.

274 Since all analysis sites are in type B site, the trend of ground motion variation to surface is very similar, so the  
 275 average values may be crucial for better implementation of the scenario-based seismic risk in the study area.  
 276 Ground response parameters such as the PGA and response spectrum intensity including the Arias intensity  
 277 show linear variation for aggregated values while increasing intensity of earthquake shaking corresponding to a  
 278 given soil profile. The mean, median, and standard deviation of the output parameters are computed. The  
 279 response spectrum intensity is computed based on Housner approach (Housner, 1959) as integral from 0.1 to 2.5  
 280 s of the pseudo-velocity spectrum that provides an indication of the average velocity for most civil engineering  
 281 structures. The plot of sensitivity of various input motions on amplitude parameters to different local soils for  
 282 the two zones is shown in Figs. 16 and 17.

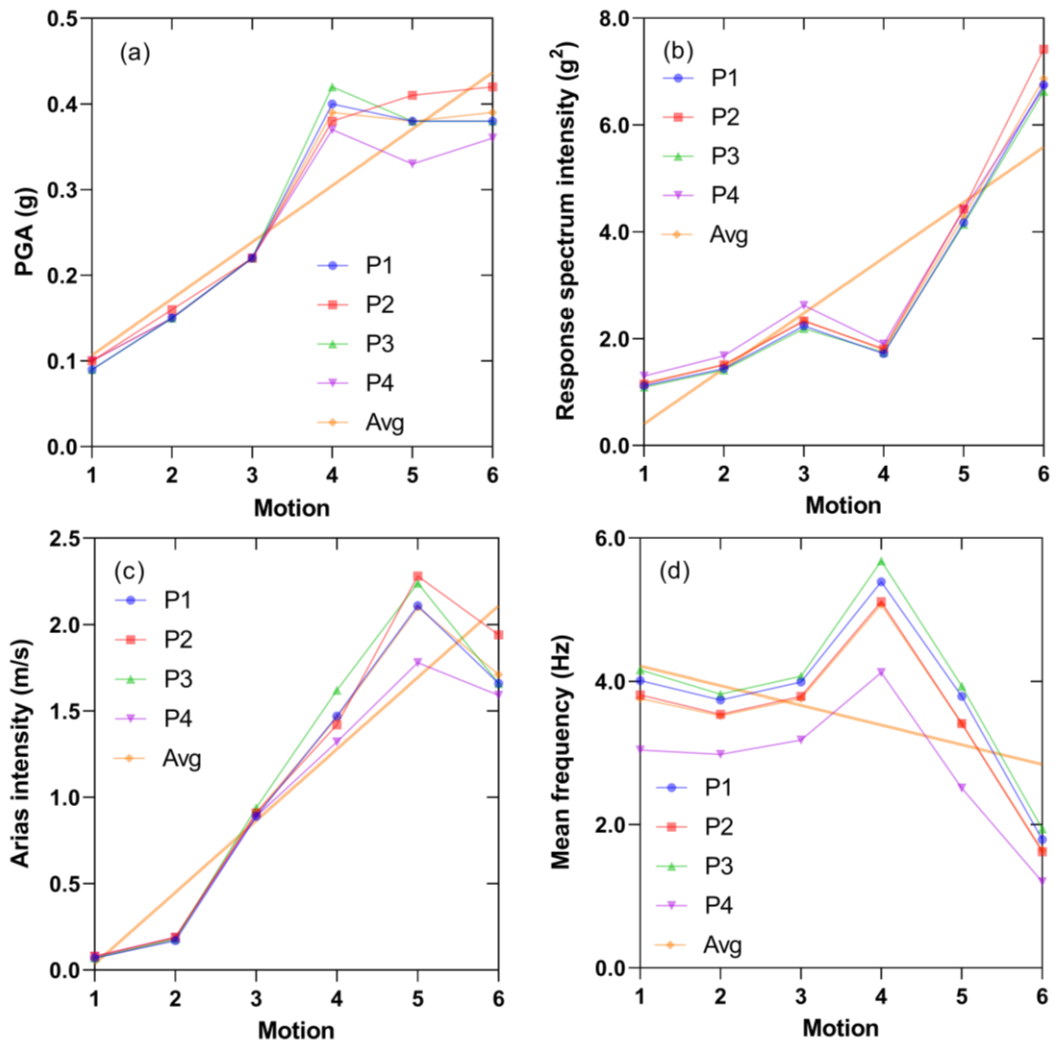
283 The standard deviation is lower for a set of predominant natural periods for a soil profile compared to  
 284 the response spectrum dataset and the deviation from the mean value indicates stronger soil response to the  
 285 SDOF systems, as shown in Table 4 and Table 5. Soil nonlinearity often shows a significant scatter in spectral  
 286 acceleration at higher and lower periods, and therefore the practical reliability of the result is that it prompts  
 287 more analysis with many input motions to predict the mean (or median) response with some level of confidence  
 288 (Kramer et al., 2012). The sensitivity of input motion is shown in Figs. 14 and 15 from two investigated  
 289 locations. The results of the correlation analysis and the sensitivity plots indicate that the input motion M4  
 290 (Northridge) has a significant influence on most of the response parameters. The additional ground response  
 291 parameters are provided in Table S1 and Table S2.

292 **Table 4.** Descriptive statistics for averaged ground response parameters in Zone I for all four soil profiles and  
 293 six input ground motions.

	PGA (g)	Arias intensity (m/sec)	Response spectrum intensity (g <sup>2</sup> )	Predominant period (sec)	Mean frequency (Hz)
Mean	0.270	1.073	2.996	0.818	3.527
Median	0.238	0.630	2.450	0.689	3.319
Standard deviation	0.121	0.765	2.013	0.468	1.097
84 <sup>th</sup> percentile	0.407	2.215	4.541	1.251	4.824
16 <sup>th</sup> percentile	0.139	0.179	1.322	0.379	2.283

294 **Table 5.** Descriptive statistics for averaged ground motion parameters in Zone II for all four soil profiles and six  
 295 input ground motions.

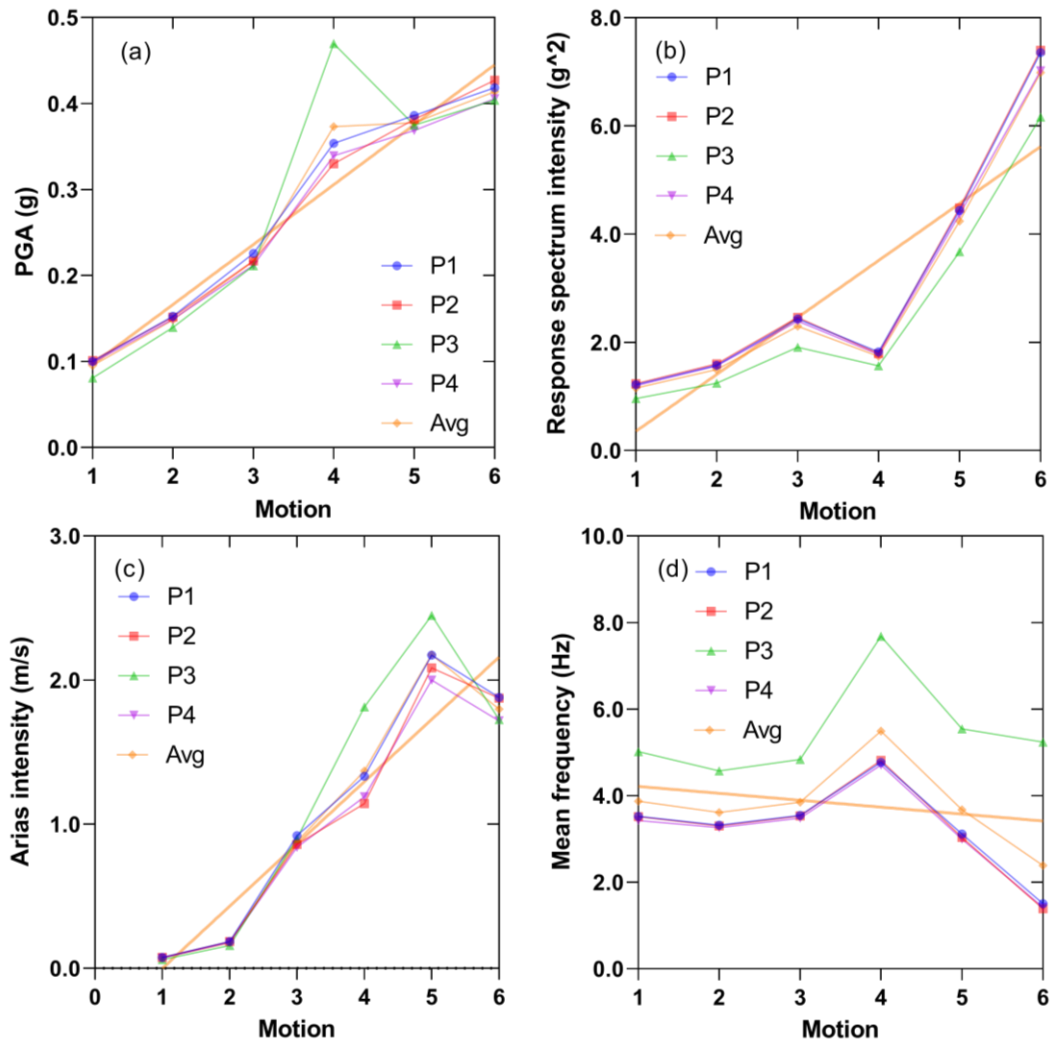
	PGA (g)	Arias intensity (m/s)	Response spectrum intensity (g <sup>2</sup> )	Predominant period (s)	Mean frequency (Hz)
Mean	0.271	1.079	2.985	0.812	3.814
Median	0.237	0.622	2.417	0.684	3.538
Standard deviation	0.126	0.794	2.066	0.453	1.382
84 <sup>th</sup> percentile	0.411	2.226	4.541	1.243	5.330
16 <sup>th</sup> percentile	0.136	0.174	1.287	0.377	2.349



296

297 **Figure 16:** Sensitivity of input ground motion in Zone I. (a) Peak ground acceleration, (b) Response spectrum  
 298 intensity, (c) Arias intensity, (d) Mean frequency. Soil profiles P1: Toorsa II, P2: Toorsa 1, P3: Dhamdhara II  
 299 and P4: Dhamdhara I.

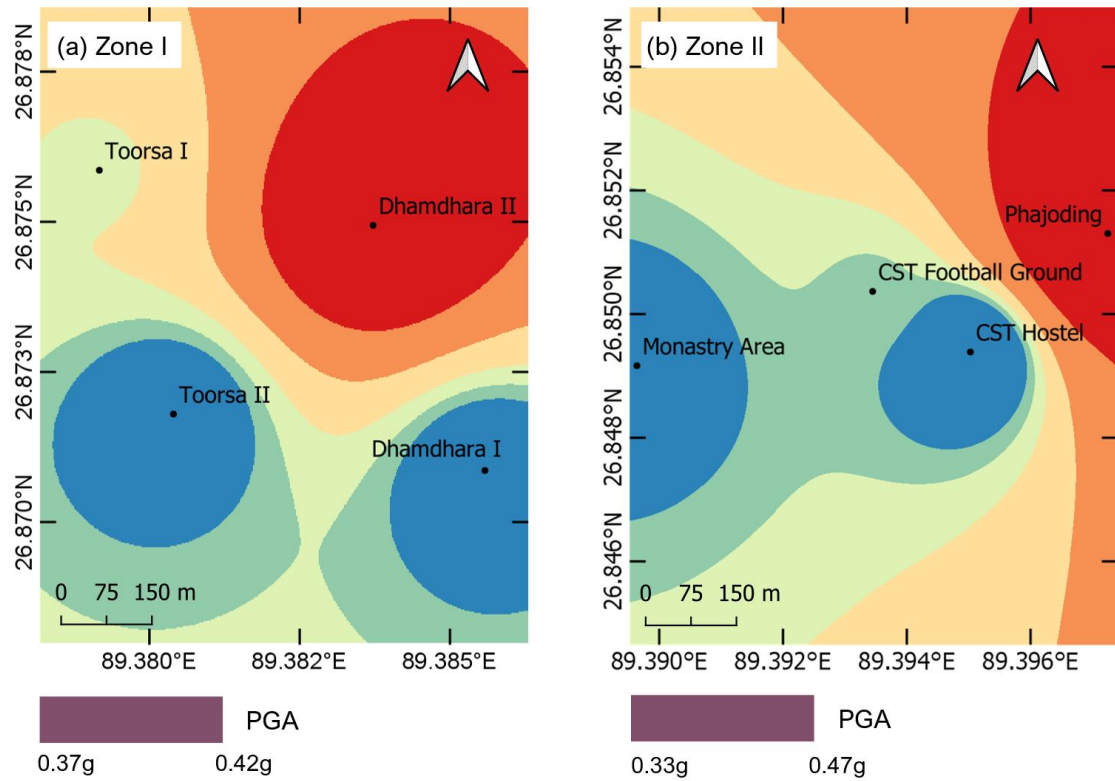
300



301

302 **Figure 17:** Sensitivity of input ground motion in Zone II. (a) Peak ground acceleration, (b) Response spectrum  
 303 intensity, (c) Arias intensity, (d) Mean frequency. Soil profiles P1: CST Football Ground, P2: CST Hostel, P3:  
 304 Phajoding, and P4: Monastery area

305 The PGA of M4 (Northridge) are mapped to show the spatial variability in two zones as shown in Fig.  
 306 18. The PGA in Zone I is distributed between 0.37 g to 0.42 g. The variability of PGA in Zone II is higher  
 307 compared to Zone I as the PGA range for Zone II is 0.33 g to 0.47 g. The resulting interplay of strong ground  
 308 motion parameters with local soil conditions primarily highlights the importance of input motion  
 309 characterization.



310

311 **Figure 18:** PGA distribution map of input motion M4 Northridge earthquake, (a) Toorsa and Dhamdhara in  
 312 Zone I, (b) Rinchening in Zone II.

313 **5. Conclusions**

314 Using 1D site response analysis, we performed sensitivity of various input motions. Ground motion parameter  
 315 sensitivity for soft soil deposits is assessed considering typical eastern Himalayan setting. Aiming to quantify  
 316 the variation of input motion characteristics, we assessed several ground motion parameters. The conclusions of  
 317 the study can be depicted as follows:

- 318 • The trend in the variation of ground motion parameters such as PGA, PGD, PGV, and SA projects an  
 319 increasing order with ground motion intensity as expected. However, the ground motions with input PGA  
 320 greater than 0.34g and less than 0.1g are more sensitive than the others. This concludes that sensitivity is  
 321 more prominent in low and high PGA range than the moderate shaking scenario (0.1-0.34g).
- 322 • For loose soil sites characterized as type B ground, peak spectral acceleration is prominent between 0.3 to 3  
 323 sec, this implies that the structures with their fundamental vibration period between 0.3 to 3 sec will  
 324 observe greater peak spectral acceleration. Consideration of earthquake resistant design for the structures  
 325 with fundamental vibration period requires additional attention due to the severity in peak spectral  
 326 acceleration occurrence.
- 327 • In general, the peak amplification factor is obtained up to 6.2 for the study area. The lower amplification  
 328 factor coincides the occurrence of bedrock early. Meanwhile, the soil columns with greater depth of loose  
 329 soil deposits have reflected greater amplification. The spatial variation of amplification factor is quite  
 330 significant even in a small area. Thus, more rigor is necessitated for site response analysis and  
 331 microzonation studies in soft soil deposits to incorporate the spatial variation in soil columns. If soil



332 stiffness is increased, the amplification factor can be checked, thus, soil improvement may be required to  
333 assure foundation performance in loose soil deposit.

334 This study uses various strong motions to depict the variability ground motion characteristics. Although this is  
335 one of the first studies in the area, the results are still preliminary and detailed investigation using sophisticated  
336 soil characteristics and approaches could effectively in obtaining more reliable results.

#### 337 **Data availability**

338 All the data used in this study are presented in the paper.

#### 339 **Author contribution**

340 Conceptualization (KT), Data curation (KT), Formal analysis (KT), Funding acquisition (KRA), Methodology  
341 (KT, DG and GF), Resources (KT, DG and KRA), Software and visualization (KT), Writing – original draft  
342 preparation (KT), Writing – review & editing (DG, NC, GF and KRA).

#### 343 **Competing interests**

344 The authors declare that they have no competing interests.

#### 345 **Acknowledgements**

346 The authors are thankful to Phuentsholing Thromde (Municipal office) for providing additional geotechnical  
347 data.

#### 348 **References**

349 Berthet, T., Hetényi, G., Cattin, R., Sapkota, S. N., Champollion, C., Kandel, T., Doerflinger, E., Drukpa, D.,  
350 Lechmann, S., and Bonnin, M.: Lateral uniformity of India Plate strength over central and eastern Nepal,  
351 *Geophysical Journal International*, 195(3), 1481–1493, <https://doi.org/10.1093/gji/ggt357>, 2013.

352 Bhutani, M., and Naval, S.: Preliminary amplification studies of some sites using different earthquake motions,  
353 *Civil Engineering Journal (Iran)*, 6(10), 1906–1921, <https://doi.org/10.28991/cej-2020-03091591>, 2020.

354 Bommer, J. J., and Martinez-Pereira, A.: Strong-motion parameters: definition, usefulness and predictability,  
355 12th World Conference on Earthquake Engineering, 1–8, <http://www.iitk.ac.in/nicee/wcee/article/0206.pdf>,  
356 2000.

357 Bradley, B. A.: Empirical correlation of PGA, spectral acceleration and spectrum intensities from active shallow  
358 crustal earthquakes, *Earthquake Engineering and Structural Dynamics*, 40(15), 1–15.  
359 <https://doi.org/10.1002/eqe>, 2011.

360 Chavez-Garcia, F. J., Pedotti, G., Hatzfeld, D., and Bard, P. Y.: An experimental study of site effects near  
361 Thessaloniki (northern Greece), *Bulletin - Seismological Society of America*, 80(4), 784–806, 1990.

362 Chettri, N., Gautam, D., and Rupakhety, R.: From Tship Chim to Pa Chim: Seismic vulnerability and  
363 strengthening of Bhutanese vernacular buildings, In R. Rupakhety and D.Gautam (Ed.), *Masonry Construction*

364 in Active Seismic Regions (1st ed. Ca, Issue May, pp. 253–288), Elsevier, [https://doi.org/10.1016/c2019-0-](https://doi.org/10.1016/c2019-0-02453-3)  
365 02453-3, 2021. a

366 Chettri, N., Gautam, D., and Rupakhety, R.: Seismic vulnerability of vernacular residential buildings in Bhutan,  
367 *Journal of Earthquake Engineering*, 26(1), 1–16. <https://doi.org/10.1080/13632469.2020.1868362>, 2021. b

368 Darendeli, M. B.: Development of a New Family of Normalized Modulus Reduction and Material Damping  
369 Curves, Dept. of Civil Eng., Univ. of Texas, Austin, 2001

370 Dobry, R., and Vucetic, M.: Dynamic properties and seismic response of soft clay deposits, *International*  
371 *Symposium on Geotech., Eng. of Soft Soils, Mexico*, 2(January 1987), 51–87, 1982.

372 Douglas, J.: Selection of strong-motion records for use as input to the structural models of VEDA, BRGM,  
373 2006.

374 Drukpa, D., Velasco, A. A., and Doser, D. I.: Seismicity in the Kingdom of Bhutan (1937-2003): Evidence for  
375 crustal transcurrent deformation, *Journal of Geophysical Research: Solid Earth*, 111(6), 1–14,  
376 <https://doi.org/10.1029/2004JB003087>, 2006.

377 EduPro Civil Systems Inc.: ProShake: Ground Response Analysis Program 2.0, User’s Manual. 2017.

378 Gautam, D.: Mapping surface motion parameters and liquefaction susceptibility in Tribhuvan International  
379 Airport, Nepal, *Geomatics, Natural Hazards and Risk*, 8(2), 1173–1184,  
380 <https://doi.org/10.1080/19475705.2017.1305993>, 2017.

381 Gautam, D., and Chamlagain, D.: Preliminary assessment of seismic site effects in the fluvio-lacustrine  
382 sediments of Kathmandu valley, Nepal, *Natural Hazards*, 81(3), 1745–1769, [https://doi.org/10.1007/s11069-](https://doi.org/10.1007/s11069-016-2154-y)  
383 016-2154-y, 2016.

384 Gautam, D., Forte, G., and Rodrigues, H.: Site effects and associated structural damage analysis in Kathmandu  
385 Valley, Nepal. *Earthquake and Structures*, 10(5), 1013–1032, <https://doi.org/10.12989/eas.2016.10.5.1013>,  
386 2016.

387 Housner, G.W.: Behavior of structures during earthquakes, *Journal of the Engineering Mechanics Division*,  
388 *ASCE*, 85(14), 109-129, 1959.

389 ISSMGE.: Manual for zonation on seismic geotechnical hazards. In: Technical committee for earthquake  
390 geotechnical engineering, TC4, international society for soil mechanics and geotechnical engineering, The  
391 Japanese Geotechnical Society, Tokyo, 1999.

392 IS:1893.: Criteria for Earthquake Resistant Design of Structures - General Provisions and Buildings Part-1,  
393 Bureau of Indian Standards, New Delhi, Part 1, 1–39, 2002.

394 Jishnu, R. B., Naik, S. P., Patra, N. R., and Malik, J. N.: Ground response analysis of Kanpur soil along Indo-  
395 Gangetic Plains, *Soil Dynamics and Earthquake Engineering*, 51(2013), 47–57,  
396 <https://doi.org/10.1016/j.soildyn.2013.04.001>, 2013.

397 Kirtas, E., Koliopoulos, P., Kappos, A., Theodoulidis, N., Savvaidis, A., Margaritis, B., and Rovithis, E.:  
398 Identification of earthquake ground motion using site effects analysis in the case of Serres city, Greece,  
399 International Journal of Civil Engineering and Architecture, 2(1), 20–27, 2015.

400 Kramer, S. L.: Geotechnical Earthquake Engineering, Prentice Hall, 1996.

401 Kramer, S. L., Arduino, P., and Sideras, S. S.: Earthquake ground motion selection, The State of Washington  
402 Department of Transportation, 2012.

403 Long, S., and McQuarrie, N.: Placing limits on channel flow: Insights from the Bhutan Himalaya, Earth and  
404 Planetary Science Letters, 290(3–4), 375–390, <https://doi.org/10.1016/j.epsl.2009.12.033>; 2010.

405 Lopez-Caballero, F., Gelis, C., Regnier, J., and Bonilla, L. F.: Site response analysis including earthquake input  
406 ground motion and soil dynamic properties variability, 15th World Conference on Earthquake Engineering,  
407 2012.

408 Licata, V., Forte, G., d’Onofrio, A., Santo, A., Silvestri, F.: A multi-level study for the seismic microzonation of  
409 the Western area of Naples (Italy), Bulletin of Earthquake Engineering, 17(9), 4711–4741, 2019.

410 McQuarrie, N., Long, S. P., Tobgay, T., Nesbit, J. N., Gehrels, G., and Ducea, M. N.: Documenting basin scale,  
411 geometry and provenance through detrital geochemical data: Lessons from the Neoproterozoic to Ordovician  
412 Lesser, Greater, and Tethyan Himalayan strata of Bhutan, Gondwana Research, 23(4), 1491–1510,  
413 <https://doi.org/10.1016/j.gr.2012.09.002>, 2013.

414 Naik, S. P., and Patra, N. R.: Generation of Liquefaction Potential Map for Kanpur City and Allahabad City of  
415 Northern India: An Attempt for Liquefaction Hazard Assessment, Geotechnical and Geological Engineering,  
416 36(1), 293–305, <https://doi.org/10.1007/s10706-017-0327-4>, 2018.

417 Nath, S. K., and Thingbaijam, K. K. S.: Seismic hazard assessment - A holistic microzonation approach, Natural  
418 Hazards and Earth System Science, 9(4), 1445–1459, <https://doi.org/10.5194/nhess-9-1445-2009>, 2009.

419 Panjamani, A., Katukuri, A. K., Reddy, G. R., Moustafa, S. S. R., and Al-Arifi, N. S. N.: Seismic site  
420 classification and amplification of shallow bedrock sites, PLoS ONE, 13(12), 1–22,  
421 <https://doi.org/10.1371/journal.pone.0208226>, 2018.

422 Puri, N., Jain, A., Mohanty, P., and Bhattacharya, S.: Earthquake Response Analysis of Sites in State of Haryana  
423 using DEEPSOIL Software, Procedia Computer Science, 125(January), 357–366,  
424 <https://doi.org/10.1016/j.procs.2017.12.047>, 2018.

425 Seed, H. B., and Idriss, I. M.: Soil Moduli and Damping Factors for Dynamic Response Analyses [Report No.  
426 EERC 70-10], Earthquake Engineering Research Centre, University of California, Berkeley,  
427 <https://ntrl.ntis.gov/NTRL/dashboard/searchResults/titleDetail/PB197869.xhtml>, 1970.

428 Seed, H. B., Wong, R. T., Idriss, I. M., and Tokimatsu, K.: Moduli and Damping Factors for Dynamic Analyses  
429 of Cohesionless Soils, Journal of Geotechnical Engineering, 112(11), 1016–1032, 1986.

430 Shafiee, A., Kamalian, M., Jafari, M. K., and Hamzehloo, H.: Ground motion studies for microzonation in Iran,  
431 *Natural Hazards*, 59(1), 481–505, <https://doi.org/10.1007/s11069-011-9772-1>, 2011.

432 Shiuly, A., and Narayan, J. P.: Deterministic seismic microzonation of Kolkata city. *Natural Hazards*, 60(2),  
433 223–240, <https://doi.org/10.1007/s11069-011-0004-5>, 2012.

434 Sil, A., and Haloi, J.: Site-specific ground response analysis of a proposed bridge site over Barak River along  
435 Silchar Bypass Road, India, *Innovative Infrastructure Solutions*, 3(1), [https://doi.org/10.1007/s41062-018-0167-](https://doi.org/10.1007/s41062-018-0167-y)  
436 *y*, 2018.

437 Sitharam, T. G.: Seismic Microzonation: Principles, Practices and Experiments, *Electronic Journal of*  
438 *Geotechnical Engineering*, 1–58, 2008.

439 Sitharam, T. G., Anbazhagan, P., Mahesh, G. U., Bharathi, K., and Reddy, P. N.: Seismic Hazard Studies Using  
440 Geotechnical Borehole Data and GIS, *Symposium on Seismic Hazard Analysis and Microzonation*, 341–358,  
441 2005.

442 Stevens, V. L., De Risi, R., Le Roux-Mallouf, R., Drukpa, D., and Hetényi, G.: Seismic hazard and risk in  
443 Bhutan, *Natural Hazards*, 104(3), 2339–2367, <https://doi.org/10.1007/s11069-020-04275-3>, 2020.

444 Tempa, K., and Chettri, N.: Comprehension of Conventional Methods for Ultimate Bearing Capacity of Shallow  
445 Foundation by PLT and SPT in Southern Bhutan, *Civil Engineering and Architecture*, 9, 375–385,  
446 <https://doi.org/10.13189/cea.2021.090210>, 2021.

447 Tempa, K., Chettri, N., Gurung, L., and Gautam, D.: Shear wave velocity profiling and ground response analysis  
448 in Phuentsholing, Bhutan, *Innovative Infrastructure Solutions*, 6(2), 1–16, [https://doi.org/10.1007/s41062-020-](https://doi.org/10.1007/s41062-020-00420-w)  
449 *00420-w*, 2021.

450 Tempa, K., Chettri, N., Sarkar, R., Saha, S., Gurung, L., Dendup, T., and Nirola, B. S.: Geotechnical parameter  
451 assessment of sediment deposit: A case study in Pasakha, Bhutan, *Cogent Engineering*, 8(1), 1–21,  
452 <https://doi.org/10.1080/23311916.2020.1869366>, 2021.

453 Tempa, K., Sarkar, R., Dikshit, A., Pradhan, B., Simonelli, A. L., Acharya, S., and Alamri, A. M.: Parametric  
454 study of local site response for bedrock ground motion to earthquake in Phuentsholing, Bhutan, *Sustainability*  
455 (Switzerland), 12(13), 1–20, <https://doi.org/10.3390/su12135273>, 2020.

456 Vucetic, M., and Dobry, R.: Effect of Soil Plasticity on Cyclic Response. *Journal of Geotechnical Engineering*,  
457 117(1), 89–107, <http://sokocalo.engr.ucdavis.edu/~jeremic/PAPERSlocalREPO/CM1769.pdf>, 1991.

458 Wyss, M., and Rosset, P.: Mapping seismic risk: The current crisis. *Natural Hazards*, 68(1), 49–52,  
459 <https://doi.org/10.1007/s11069-012-0256-8>, 2013.

460 Zafarani, H., Ghafoori, S. M. M., Soghrat, M. R., and Shafiee, M.: Spatial correlation of peak ground motions  
461 and pseudo-spectral acceleration based on the sarpol-e-zahab mw 7.3, 2017 earthquake data, *Annals of*  
462 *Geophysics*, 63(4), 1–15, <https://doi.org/10.4401/ag-8349>, 2020.